

## Stressed Fibonacci spiral patterns of definite chirality

Chaorong Li

Zhejiang Sci-Tech University, Hangzhou 310018, China and Institute of Physics, P.O. Box 603, Beijing 100080, China

Ailing Ji and Zexian Cao<sup>a)</sup>

Beijing National Laboratory for Condensed Matter Physics, Institute of Physics, Chinese Academy of Sciences, P.O. Box 603, Beijing 100080, China

(Received 21 August 2006; accepted 22 February 2007; published online 18 April 2007)

Fibonacci spirals are ubiquitous in nature, but the spontaneous assembly of such patterns has rarely been realized in laboratory. By manipulating the stress on Ag core/SiO<sub>2</sub> shell microstructures, the authors obtained a series of Fibonacci spirals (3 × 5 to 13 × 21) of definite chirality as a least elastic energy configuration. The Fibonacci spirals occur uniquely on conical supports-spherical receptacles result in triangular tessellations, and slanted receptacles introduce irregularities. These results demonstrate an effective path for the mass fabrication of patterned structures on curved surfaces; they may also provide a complementary mechanism for the formation of phyllotactic patterns.

© 2007 American Institute of Physics. [DOI: 10.1063/1.2728578]

Fibonacci spiral patterns are a configuration that curves both clockwise and counterclockwise, and the numbers of the spirals are the two neighbors from the Fibonacci series 1, 1, 2, 3, 5, 8, 13, 21, 34, ...<sup>1</sup> Such spiral patterns as an ordered packing can be found in every corner of the world of plants, and they are highly appreciated largely due to the innumerable amazing properties of the Fibonacci series. Efficiency principle and aesthetic considerations provide an intuitive explanation to the preferential occurrence of Fibonacci spirals in nature; for scientists, there must be a working principle, essentially mathematical and physical,<sup>2-7</sup> following which such a pattern can be precisely reproduced. In 1992, Douady and Couder succeeded in obtaining some Fibonacci spirals with drops of ferrofluid under a magnetic field, showing that the formation of Fibonacci spirals in plants might be a dynamic self-organizing process.<sup>2</sup> By deforming metal shells and rings, Steele generated some Fibonacci spiral-like patterns as least elastic energy configurations.<sup>6</sup> Remarkably, the initiative that plant patterns including the Fibonacci spirals may result from the effort to minimize the total elastic energy appears time and again in literature,<sup>8-11</sup> and the adherence of the plant pattern to the geometry of the support (receptacle, in botanic terminology) was perceived by Richards in 1948<sup>12</sup> and reemphasized by Mitchison in 1977.<sup>4</sup> However, there are no experimental evidences that the Fibonacci spirals can be systematically reproduced in a simply stressed structure of inorganic materials.

Stress engineering is a technique recently devised for the mass fabrication of ordered micro- and nanostructures.<sup>13-20</sup> In an elastically mismatched structure comprising a stiff layer on compliant substrate, a rich variety of buckling modes have been realized by adjusting the mechanical parameters and the geometry of the system. With a well-controlled experiment, a one-dimensional undulated buckling mode was obtained, and the gold nanowires grown on such a template measure 3.0 mm long.<sup>18</sup> Since the governing equations for a stressed system, i.e., the Föppl-von Kármán

equations, are fourth-order differential equations, a variety of totally different buckling modes can be fabricated by modifying the boundary and/or pinning conditions.<sup>14</sup> Inspired by the achievements made on planar surfaces, we tried to manipulate the stress patterns on a curved surface, in the hope of obtaining some ordered structures for application. In doing so, inorganic Ag core/SiO<sub>2</sub> shell microstructures of varying shapes were prepared to reveal the most stressed sites in a least elastic energy configuration. We reproduced four sets of Fibonacci spiral patterns specified as 3 × 5 to 13 × 21, and in both sinister and dexter forms.

The Ag core/SiO<sub>2</sub> shell microstructures were prepared onto the polycrystalline-Al<sub>2</sub>O<sub>3</sub> substrates by coevaporating a mixed powder of Ag<sub>2</sub>O and SiO in various mass ratios, with the substrates placed at ~1.0 cm above the source. For the core/shells presented in this letter, the mass ratio of Ag<sub>2</sub>O versus SiO was varied between 2:1 and 1:1. The substrates were primarily held at 1270 K, a temperature deliberately chosen to be slightly above the melting point of silver (1234.8 K) but far below that of SiO<sub>2</sub> (1883 K) in order to provide a favorite condition for the formation of Ag core/SiO<sub>2</sub> shells. With the given processing parameters, the thickness of the SiO<sub>2</sub> shell was maintained at below 150 nm. The two materials have significantly different thermal expansion coefficients at 1270 K,  $\alpha_{\text{SiO}_2} = 0.45 \times 10^{-6}/\text{K}$  and  $\alpha_{\text{Ag}} = 27.1 \times 10^{-6}/\text{K}$ ; hence a large stress is developed upon cooling in the shell, as given in the formula  $\sigma = [E_{\text{SiO}_2}(\alpha_{\text{Ag}} - \alpha_{\text{SiO}_2}) / (1 - \nu_{\text{SiO}_2})] \Delta T$ , where  $E_{\text{SiO}_2} = 75 \times [1 + 1.5 \times 10^{-4}(T - 15.0)]$  is the elastic modulus in gigapascal for SiO<sub>2</sub> and  $\nu_{\text{SiO}_2} = 0.17$  is Poisson's ratio. In case the thermal stress exceeds a critical value  $\sigma_c$  (for a spherical shell,  $\sigma_c = [E_{\text{SiO}_2} / \sqrt{3(1 - \nu_{\text{SiO}_2}^2)}](t/R)$ , where  $t$  is the shell thickness and  $R$  the shell radius<sup>21</sup>), the SiO<sub>2</sub> shell will become unstable against the formation of buckling modes. The stressed patterns were made observable through the subsequent biased growth of spherules onto the most stressed sites at the later stage of cooling. Ex situ observation of the patterns was performed on a scanning electron microscope (FEI, Serion) operated at 5.0 keV.

<sup>a)</sup> Author to whom correspondence should be addressed; electronic mail: zxcao@aphy.iphy.ac.cn

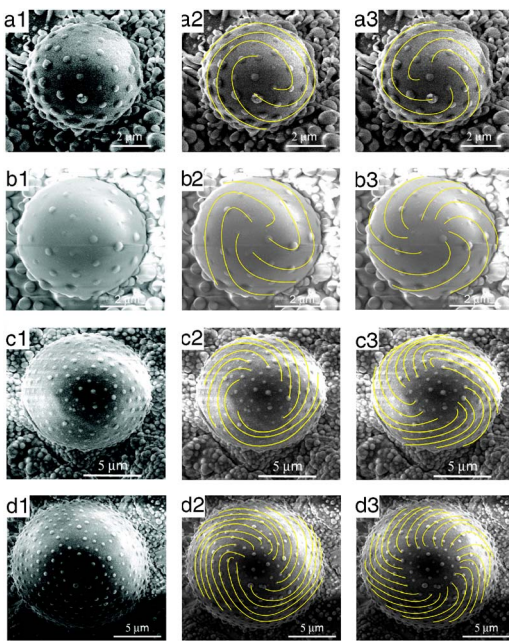


FIG. 1. Fibonacci spiral patterns in the sinister form grown on Ag core/SiO<sub>2</sub> shell microstructures: (a)  $3 \times 5$ , (b)  $5 \times 8$ , (c)  $8 \times 13$ , and (d)  $13 \times 21$ . Each individual pattern is presented in triad, one original and two with plotted counterclockwise and clockwise spirals to guide the eyes.

In different wetting conditions onto the substrate, the free surface of the Ag core/SiO<sub>2</sub> shell microstructures brings about the presence of an apex as antipode to the contact point. Since the substrate was held horizontal, axisymmetrical core/shells were obtained, with the axis of symmetry lying along the direction of gravitation, that near the apices they can be approximated with a paraboloid of revolution. In Fig. 1, the decorating spherules that reveal the most stressed sites on the primary core/shells manifest obviously parastichous spirals. With little effort we identified the Fibonacci spiral patterns as  $3 \times 5$ ,  $5 \times 8$ ,  $8 \times 13$ , and  $13 \times 21$ . The numbers of spherules visible to the reader are roughly of 40, 126, 150, and 290, respectively. These are the only four sets of Fibonacci spiral patterns realizable in the current experimental system, since, by rough estimation based on the property of Fibonacci series, the next Fibonacci spiral pattern,  $21 \times 34$ , requires more than 700 spherules, which is prohibitive for a micro-sized Ag core/SiO<sub>2</sub> shell—the large stress demanded to generate so dense a buckling mode would bring the core/shell structure to crash.

The stressed Fibonacci patterns have grown both in the sinister form (spirals in large number run counterclockwise) and in the dexter form (spirals in large number run clockwise), as in pine cones.<sup>22</sup> In Fig. 1, all the four Fibonacci patterns are in the dexter form. For all but the last one, their sinister counterparts were also obtained (Fig. 2). From the current experiment, we cannot figure out a biasing factor that predetermines the chirality for the spiral patterns. It is believed that they occur in plants at random;<sup>22</sup> but, when modeled as a least energy configuration for confined particles (see below), there may be a factor, geometrical in nature, that tips the balance.

In the case that the primary Ag core/SiO<sub>2</sub> shells exhibit a worse wetting to the substrate, they adopt a nearly spherical shape. Accordingly, the spherules arrange themselves into a quite perfect triangular tessellation, i.e., triangular lattice with a proper number of fivefold disclinations (Fig. 3). This

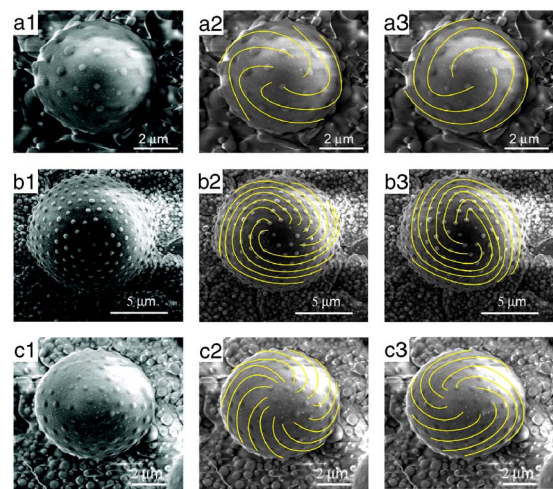


FIG. 2. Fibonacci spiral patterns in the dexter form: (a)  $3 \times 5$ , (b)  $5 \times 8$ , and (c)  $8 \times 13$ .

reminds us of the famous Thomson's problem concerning the least energy configuration of identical charges on the surface of a conducting sphere.<sup>23</sup> In fact, our stressed patterns on the nearly spherical supports fit very well with the numerical solutions to Thomson's problem. This strongly suggests that the stressed patterns on a homogeneous spherical surface as a least elastic energy configuration can be modeled with mutually repulsive charges, though the interactions involved in the two circumstances differ a lot. The robustness of the ultimate least energy configurations against the concrete interaction is a well-established fact on both the planar and the spherical surfaces,<sup>23–26</sup> even though it lacks a rigorous mathematical proof. In fact, they have been verified in diverse physical systems including the two-dimensional electron gas and the magnetic flux in superconductors,<sup>25,26</sup> to name only a few, where the form of the potentials and the number of particles show significant differences.

Since the triangular tessellation in Figs. 3(a) and 3(b) and the Fibonacci spirals in Figs. 1 and 2 result from the

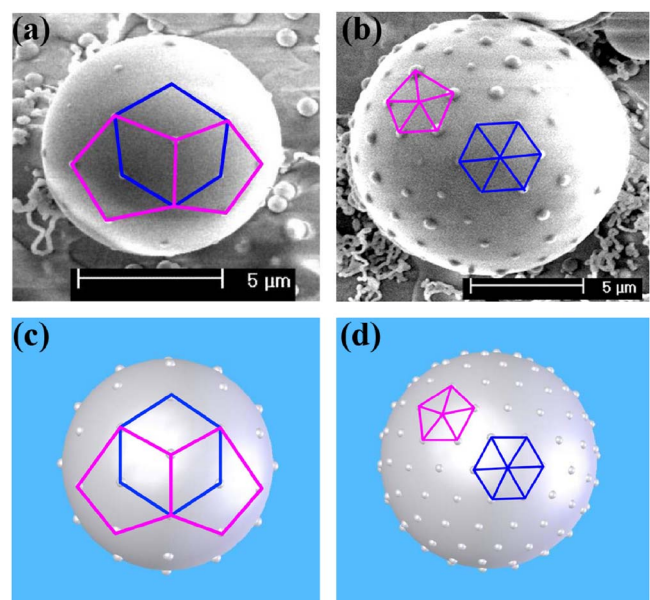


FIG. 3. Patterns on spherical supports. (a) and (b) are stressed patterns, and (c) and (d) illustrate the numerical solutions to Thomson's problem of  $N = 46$  and  $140$  (Courtesy of Bowick, see Ref. 24), respectively.



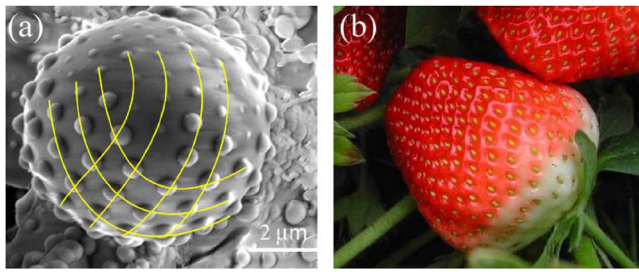


FIG. 4. Parastichous spirals on frustrating surfaces. (a) Stressed pattern on a slanted Ag core/SiO<sub>2</sub> shell microstructure, and (b) the “X pattern” of achenes in a strawberry.

same experiment, we believe that the formation of the Fibonacci spirals might as well be modeled by mutually repulsive particles but on a conical surface. That the stressed Fibonacci spirals come about on conical supports without rigorous request on the degree of perfection or the magnitude of conicity, as observed in this experiment on a dozen of core/shell microstructures of differing sizes and/or shell thicknesses, confirms the robustness of the Fibonacci spiral pattern, which might explain its wide spreading in the kingdom of plants.<sup>4</sup> This is quite easy to understand since it is analogous to the robustness of the triangular lattices for planar surfaces and the triangular tessellations for spherical surfaces. Modeled as least energy configuration for a collection of mutually repulsive entities, the stressed patterns will remain congruent so long as the confining support maintains its geometric features, and it is conceivable that a marked departure from those patterns of high regularity occurs in assemblies grown on a frustrating surface where the symmetry is broken.<sup>27</sup> To demonstrate this, some core/shells were prepared with the substrate slightly kipped so as to eliminate the axisymmetry. The spherules thereupon are found falling into parastichous spirals though, but showing a frustration here and there [Fig. 4(a)]. The situation is quite similar to that in a ripe strawberry where the axisymmetry is usually missing and consequently the achenes are disposed in the typical “X pattern” [Fig. 4(b)]. In fact, strawberry provides an illustrating example of the receptacle-shaped pattern transition that, with its softish receptacle transforming from a disk as that of a sunflower through a green cone into an asymmetrical ripe pseudocarp, the pattern changes readily from the Fibonacci spirals for florets into the X pattern for achenes.

By now, we have prepared core/shells in various shapes: from the nearly spheres, through the “conical” ones of varying conicity, to those being conical by and large but with the axisymmetry in absence. Accordingly, the stressed patterns are triangular tessellation with disclinations,<sup>15</sup> Fibonacci spiral patterns of definite chirality, and the so-called X pattern. The adherence of the Fibonacci spiral patterns to the conical supports is strikingly robust. This observation reinforces the “geometry of phyllotaxis” revealed by Richards,<sup>12</sup> and can be suggestive for the design of self-assembled structures on curvy surfaces. In an inhomogeneous mechanical system, stressed Fibonacci spiral patterns might occur on a spherical or cylindrical support, which only needs be conical when weighted with the local mechanical constants. At the moment, we cannot give a strict proof of this conjecture; even numerical tests should also wait for some time, considering the very slow progress with the much simpler Thomson’s

problem. Fortunately, many confirmative evidences can be found in nature. For example, the flower heads for both dandelion and dahlia are nearly spherical; however, the seeds of dandelion that grow simultaneously are packed in triangular tessellation, whereas the successively growing florets on dahlia fall into spirals.

In summary, we demonstrated that the Fibonacci spiral patterns of definite chirality can be reproduced through stress manipulation on the Ag core/SiO<sub>2</sub> shell microstructures. These results will be very helpful for the design and fabrication of patterned structures on curved surfaces that can find useful applications in photonics and foldable electronics. Furthermore, these results obtained in a purely inorganic material system hint at the role of stress in influencing the plant patterns. We speculate that the prerequisite for the occurrence of Fibonacci spiral patterns as stressed buckling modes be the availability of a conical support. The robust adherence of the stressed patterns to the geometry of the supports sheds some light on the mechanical rationale underlying the formation of particular plant patterns. Of course, a comprehensive model for the formation of plant patterns should incorporate as well the biochemical and genetic processes that alter growth at deeper levels.

This work was supported by the National Natural Science Foundation of China and the Space Exploration Program of China.

<sup>1</sup>The website <http://www.mscs.dal.ca/Fibonacci/> provides extensive information about the Fibonacci series and their ubiquity in the world of plants.

<sup>2</sup>S. Douady and Y. Couder, *Phys. Rev. Lett.* **68**, 2098 (1992).

<sup>3</sup>H. Meinhardt, *Models of Biological Pattern Formation* (Academic, London, 1982).

<sup>4</sup>G. J. Mitchison, *Science* **196**, 270 (1977).

<sup>5</sup>I. Adler, D. Barabe, and R. V. Jean, *Ann. Bot. (London)* **80**, 231 (1997).

<sup>6</sup>C. R. Steele, *J. Appl. Mech.* **67**, 237 (2000).

<sup>7</sup>D’Arcy and W. Thompson, *On Growth and Form* (Dover, New York, 1992), Vol. 1, p. 19.

<sup>8</sup>P. B. Green, *Int. J. Plant. Sci.* **153**, S59 (1992).

<sup>9</sup>I. Adler, *J. Theor. Biol.* **45**, 1 (1974).

<sup>10</sup>R. V. Jean, *J. Theor. Biol.* **87**, 569 (1980).

<sup>11</sup>L. S. Levitov, *Europhys. Lett.* **14**, 533 (1991).

<sup>12</sup>F. J. Richards, *Symp. Soc. Exp. Biol.* **2**, 217 (1948).

<sup>13</sup>W. T. S. Huck, N. Bowden, P. Onck, T. Pardoen, J. W. Hutchinson, and G. M. Whitesides, *Langmuir* **16**, 3497 (2000).

<sup>14</sup>N. Bowden, S. Brittain, A. G. Evans, J. W. Hutchinson, and G. M. Whitesides, *Nature (London)* **393**, 146 (1998).

<sup>15</sup>X. N. Zhang, C. R. Li, Z. Zhang, and Z. X. Cao, *Appl. Phys. Lett.* **85**, 3570 (2004).

<sup>16</sup>E. Cerda and L. Mahadevan, *Phys. Rev. Lett.* **90**, 074302 (2003).

<sup>17</sup>K. Efimenko, M. Rackaitis, E. Anias, A. Vaziri, L. Mahadevan, and J. Genzer, *Nat. Mater.* **4**, 293 (2005).

<sup>18</sup>R. Adelung, O. C. Aktas, J. Franc, A. Biswas, R. Kunz, M. Elbahri, J. Kanzow, U. Schmuermann, and F. Faupel, *Nat. Mater.* **3**, 375 (2004).

<sup>19</sup>C. R. Li, X. N. Zhang, and Z. X. Cao, *Science* **309**, 909 (2005).

<sup>20</sup>X. Chen and J. W. Hutchinson, *Scr. Mater.* **50**, 797 (2004).

<sup>21</sup>S. P. Timoshenko and J. M. Gere, *Theory of Elastic Stability*, 2nd ed. (McGraw-Hill, New York, 1961), p. 512.

<sup>22</sup>A. J. S. Klar, *Nature (London)* **417**, 595 (2002).

<sup>23</sup>E. L. Altschuler, *Phys. Rev. Lett.* **78**, 2681 (1997).

<sup>24</sup>A. R. Bausch, M. J. Bowick, A. Cacciuto, A. D. Dinsmore, M. F. Hsu, D. R. Nelson, M. G. Nikolaides, A. Travesset, and D. A. Weitz, *Science* **299**, 1716 (2003).

<sup>25</sup>E. P. Wigner, *Phys. Rev.* **46**, 1002 (1934).

<sup>26</sup>H. F. Hess, R. B. Robinson, R. C. Dynes, J. M. Valles, and J. V. Waszczak, *Phys. Rev. Lett.* **62**, 214 (1989).

<sup>27</sup>K. S. Shin, H. Q. Xiang, S. I. Moon, T. H. Kim, T. J. McCarthy, and T. P. Russell, *Science* **306**, 76 (2004).